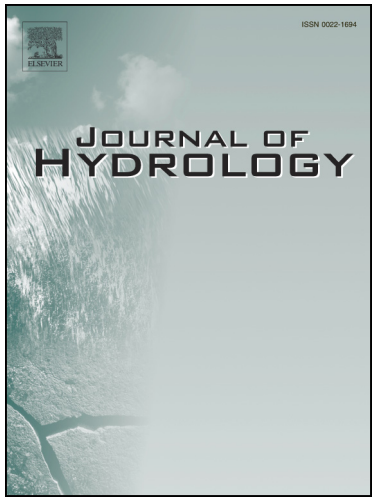

Research papers

Estimates of Gridded Relative Changes in 24-h Extreme Rainfall Intensities Based on Pooled Frequency Analysis

Ana I. Requena, Donald H. Burn, Paulin Coulibaly

PII: S0022-1694(19)30660-2
DOI: https://doi.org/10.1016/j.jhydrol.2019.123940
Article Number: 123940
Reference: HYDROL 123940

To appear in: *Journal of Hydrology*

Received Date: 12 April 2019
Revised Date: 17 June 2019
Accepted Date: 9 July 2019

Please cite this article as: Requena, A.I., Burn, D.H., Coulibaly, P., Estimates of Gridded Relative Changes in 24-h Extreme Rainfall Intensities Based on Pooled Frequency Analysis, *Journal of Hydrology* (2019), doi: https://doi.org/10.1016/j.jhydrol.2019.123940

Estimates of Gridded Relative Changes in 24-h Extreme Rainfall Intensities Based on Pooled Frequency Analysis

Ana I. Requena [1, 2 *] ORCID: 0000-0002-0438-5898, Donald H. Burn [2] ORCID: 0000-0001-7917-6380, Paulin Coulibaly [1] ORCID: 0000-0003-0227-9503

[1] Civil Engineering, McMaster University, Hamilton, Ontario, Canada. requena@mcmaster.ca; couliba@mcmaster.ca

[2] Civil and Environmental Engineering, University of Waterloo, Waterloo, Ontario, Canada. dhburn@uwaterloo.ca

* Corresponding author: Ana I. Requena; requena@mcmaster.ca

Abstract

The potential effect of climate change needs to be considered in urban infrastructure design and risk assessment to improve reliability. The present study proposes a methodology for obtaining grid-scale relative changes for updating 24-h extreme rainfall intensity, through the estimation of rainfall intensity quantiles from baseline and future simulations using a pooled frequency analysis approach. Coherence of relative changes over return periods and time horizons is analysed, and adjustments are proposed to facilitate the application of relative changes in practice. The approach is applied to Canada, using gridded daily precipitation series from model combinations belonging to the North American Coordinated Regional Climate Downscaling Experiment. Multi-model 10^{th}, 50^{th} and 90^{th} percentile relative changes are provided for six return periods, considering two future scenarios (RCP 4.5 and RCP 8.5), and two horizons (2050 and 2080). Overall, estimated relative changes varied smoothly and formed a number of clusters of similar values across the country. Relative changes for RCP 8.5 are recommended for 2050, whereas either those for RCP 4.5 or RCP 8.5 could be used for 2080. As an example, median multi-model 50th percentile relative change over Canada is found to be 14%, 16% and 27% for RCP 4.5 – 2080, RCP 8.5 – 2050, and RCP 8.5 – 2080, respectively.

Keywords: climate change; grid-scale; intensity-duration-frequency (IDF) curves; pooled frequency analysis; extreme rainfall; Canada.

1. Introduction

Urban infrastructure design and risk assessment based on observed rainfall records assumes that similar climate conditions will be experienced in the future. However, climate change due to increasing greenhouse gases challenges this assumption (e.g., Kotamarthi et al. 2016). Analyses performed at a global scale provided evidence of the effect of climate change on precipitation extremes (e.g., Wang et al. 2017; Papalexiou and Montanari 2019). Climate model simulations considering different future scenarios are a common source of information to update rainfall intensity quantiles, usually presented as intensity-duration-frequency (IDF) curves, needed in urban infrastructure design (e.g., Willems et al. 2012). Climate model simulations are usually provided at a coarse grid-scale spatial resolution by Global Climate Models (GCMs) that can be downscaled to higher resolutions by dynamic downscaling, such as through Regional Climate Models (RCMs) (e.g., Kuo et al. 2015), or by statistical downscaling (e.g., Nguyen et al. 2007; Khalili and Nguyen 2017).

Climate model simulations often present bias, which may be solved by bias correction methods, such as the well-known quantile mapping approach (e.g., Li et al. 2017; Switzman et al. 2017). To apply bias correction, climate model simulations and observations need to have a similar spatial and temporal resolution to avoid the inflation issue, which is caused by difference in scale, as a result of explaining station-scale variability with grid-scale variability (Maraun 2013; Haerter 2015). A commonly used approach is the delta change method. Although sometimes defined as a bias correction method, the delta change method does not specifically provide bias corrected series of the climate model but rather an estimate of the climate (or "delta") change between future horizon and baseline period simulations; applied to observations, it results in future projections (e.g., Maraun 2016). The underlying assumptions are the

following. Bias in baseline and future simulations is multiplicative and stationary and hence may be cancelled out when estimating the delta change (Li et al. 2015). Changes at a larger spatial scale also characterise those at a smaller spatial scale (Sunyer et al. 2015). Observation-based temporal and spatial variability is preserved (e.g., Switzman et al. 2017). The delta change method is used in local (e.g., Zhu et al. 2012; Switzman et al. 2017) and regional approaches (e.g., Ekström et al. 2005; Mladjic et al. 2011; Mailhot et al. 2012).

The use of a regional approach to estimate rainfall quantiles from either observations or climate model simulations allows obtaining more accurate estimates, especially for longer return periods (e.g., Mladjic et al. 2011; Requena et al. 2019), as well as smoother spatial patterns when estimating future changes (Li et al. 2017). Some form of fixed-region approach is used for analysing future changes in several studies (e.g., Ekström et al. 2005; Mailhot et al. 2007, 2012; Mladjic et al. 2011; Monette et al. 2012; DeGaetano et al. 2017). A pooled approach is used by Li et al. (2017), through which pooling groups of 500 grid-years are formed based on geographic proximity to estimate 24-h rainfall quantiles in the Greater Sydney region, Australia.

The present study proposes a methodology for obtaining grid-scale relative changes to update 24-h extreme rainfall intensity, based on the estimation of rainfall intensity quantiles for baseline and future periods by using pooled frequency analysis. The grid scale approach provides relative changes closer to the catchment scale, which is usually needed in practice, avoiding downscaling to the station scale for later upscaling to catchment scale. It also allows supplying results across a large study area with a low gauge density, since in that case downscaling to station scale would imply only providing relative changes where stations are available and not using the available information for the rest of the study area. Because of considering grid-scale and low gauge density, the estimation of relative changes is based on the delta change method.

Relative changes at a grid-scale based on the delta change method are provided by several studies (e.g., Ekström et al. 2005; Mladjic et al. 2011; Mailhot et al. 2012).

The present study estimates relative changes through a pooled approach rather than through a fixed-region approach as used in other large grid-scale studies. The pooled approach not only allows for a more accurate estimation of quantiles associated with longer return periods, but also for more flexibility in the formation of pooling groups for quantile estimation, avoiding marked limits between regions. The pooled approach used in this study is that recommended in Requena et al. (2019), which is focused on the gauged case; that is, on the estimation of pooled quantiles at a target site where rainfall series are available. Hence, it is in agreement with information from climate models, since precipitation simulation series are available at the target grid. The pooled approach is based on the index-event model, and the region of influence approach, with a geographic distance similarity measure. The method advocates for an increasing initial pooling group size with increases in return period, and a trade-off between pooling group size and homogeneity in pooling group formation for longer return periods. Since the approach was initially applied to observations, pooling group size was defined by number of station-years; in the present study, the approach is applied to gridded simulations and hence pooling group size is defined by number of grid-years. Once relative changes are estimated, coherence over return periods and horizons is analysed, and adjustments are proposed to facilitate their application in practice.

Simpler pooled approaches are applied to relatively small areas in other studies (e.g., Li et al. 2017). In the present study, the approach is applied to a large case study, consisting of most of Canada, where grid-scale 24-h relative changes are estimated for six return periods (2, 5, 10, 25, 50, and 100 years). Significant trends are found on observed annual maximum rainfall series

under local or regional approaches in Canada, with a larger presence of increasing trends (e.g., Burn and Taleghani 2013; Shephard et al. 2014; Requena et al. 2019). This supports the need of updating IDF curves in Canada based on climate model projections, in line with earlier studies performed at the grid scale for the country (e.g., Mladjic et al. 2011; Mailhot et al. 2012). RCMs are often considered as preferable to study extreme rainfall due to their ability to simulate mesoscale precipitation at a higher detail than GCMs (e.g., Kuo et al. 2014). Therefore, the latest RCM simulations, belonging to the North American Coordinated Regional Climate Downscaling Experiment (NA-CORDEX) are used in this study. Relative changes across Canada are estimated considering two future scenarios (Representative Concentration Pathways RCP 4.5 and RCP 8.5) and two future horizons (2050 and 2080). Results are also extracted for particular cities to provide an overview of relative changes across the country. Estimated relative changes are compared with those provided by existing studies over Canada; two studies based on a fixed-region approach and one local approach. The present study is organised as follows. Methodology is described in Section 2. Case study and data are presented in Section 3. Application to Canada is shown in Section 4. Discussion is provided in Section 5, and conclusions are given in Section 6.

2. Methodology

The procedure proposed for estimating grid-scale 24-h relative changes for extreme rainfall intensity update consists of three steps: (i) extraction of annual maximum rainfall series from grid-scale daily precipitation; (ii) pooled quantile estimation for grid-scale annual maximum rainfall intensity; and (iii) estimation of grid-scale relative changes.

2.1. Extraction of annual maximum rainfall series from grid-scale daily precipitation

The extraction of annual maximum series from climate model precipitation simulations and observations should be consistent to provide associated suitable projected changes for IDF update. In this regard, the same rainfall period needs to be considered for extraction of annual maximum rainfall series for observations and simulations. Furthermore, for cases where precipitation may occur as rainfall or snow, such as in cold and/or mountainous areas, precipitation extremes may be related to either of the two types of events. In these cases, observations are commonly associated with rainfall events (since stations are usually out of service during winter), whereas climate model precipitation simulations may correspond to rainfall or snow events. Over the literature, different approaches are considered. Mailhot et al. (2012) considered the entire year for building annual maximum precipitation series across Canada, whereas Mladjic et al. (2011) used the period April-September to avoid mixing snow and rainfall extremes across the country. Mailhot et al. (2007) and Monette et al. (2012) used the period May-October in particular case studies related to the province of Quebec, Canada.

In the present study, starting and ending months of observed rainfall are analysed to identify objective periods for annual maximum rainfall series extraction from grid-scale precipitation simulations. The analysis is performed by dividing the area of study into regions according to different administrative and climate-based classifications. The lower and upper bound of the rainfall period assigned to a given region is estimated as the 25^{th} percentile starting month and the 75^{th} percentile ending month from stations within the region, respectively. Once the main rainfall period categories are determined across the area of study, each gridpoint (i.e., center of the grid) associated with climate model simulations is linked to the main rainfall period category in which it is located. Grid-scale daily annual maximum rainfall series are then extracted from

grid-scale daily precipitation simulations using the months defined by the rainfall period category.

2.2. Pooled quantile estimation for grid-scale annual maximum rainfall intensity

The pooled estimate of the *T*-year rainfall intensity quantile is obtained following the recommendations provided by Requena et al. (2019), as a result of assessing a number of approaches for pooling group formation according to quantile estimation and uncertainty for pooled rainfall intensity frequency analysis at gauged sites. The approach is applied using "grid-years" instead of "station-years", since grid-scale instead of point-scale annual maximum rainfall intensity series are used in the present study. This allows for coherence in the estimation of both observation-based and simulation-based pooled quantiles. A summary of the pooled approach is provided below. Pooling groups are built based on the region of influence approach (Burn 1990) with the geographical distance similarity measure. The initial pooling group size, defined as the number of grid-years in a pooling group, increases with the return period according to the 5*T* guideline (Robson and Reed 1999), which suggests that the number of station-years of data in a pooling group should be at least 5 times the return period of interest. A minimum of 125 grid-years is used regardless of the return period. For long return periods (i.e., $T \geq 50$ years), a trade-off between pooling group size and homogeneity is considered. In that case, the pooling group is tested for homogeneity and the most dissimilar grid (i.e., the furthest grid) is removed from the pooling group until reaching homogeneity (i.e., the heterogeneity measure, *H,* in Hosking and Wallis 1997, being less than two), under the condition that the final pooling group contains a minimum of 125 grid-years.

The well-known index-event model (Dalrymple 1960; Hosking and Wallis 1997) is applied to the pooling group to obtain the grid-scale pooled estimate of the *T*-year rainfall intensity

quantile. For simplicity, the grid-scale pooled estimate of the *T*-year rainfall intensity quantile for the 24-h rainfall duration will be referred to as "baseline quantile", "future quantile" and "observation-based quantile", when obtained from baseline simulations, future simulations and observations, respectively.

Comparison between baseline and observation-based quantiles is performed to provide a notion of the overall ability of the ensemble of climate model simulations to estimate suitable quantiles across the study domain. For that purpose, the multi-model median baseline quantile is obtained at each grid as the median value of the ensemble of baseline quantiles estimated from each climate model. Differences among the two types of quantiles are expected (e.g., Mailhot et al. 2007; Kuo et al. 2014; Li et al. 2015), since baseline quantiles are obtained from grid-scale series (i.e., they represent "areal" intensity) and observation-based quantiles are obtained from point-series (i.e., they represent "point" intensity). In this regard, the following analysis is done, motivated by the premise that maximum areal average rates are less than maximum point rates (Fowler et al. 2005), and by the estimation of lower and upper quantile bounds from stations and grids within the city of Edmonton for the assessment of simulated IDFs in Kuo et al. (2014). The analysis consists in identifying the minimum and maximum observation-based quantile from stations within a grid, and compare this range with the (grid-scale) baseline quantile. If the baseline quantile is within the range, it is considered to be suitable and a value of 1 is assigned to the grid, being 0 otherwise. The percentage of grids fulfilling the criterion, their spatial distribution, and the relationship with gauge density is then analysed.

2.3. Estimation of grid-scale relative changes

Relative changes, C_{r}, expressed in %, are calculated at each grid as follows:

$$C_{\mathrm{r}} = \left(\frac{\hat{R}_{\mathrm{T,f}} - \hat{R}_{\mathrm{T,b}}}{\hat{R}_{\mathrm{T,b}}}\right)100 = \left(\frac{\hat{R}_{\mathrm{T,f}}}{\hat{R}_{\mathrm{T,b}}} - 1\right)100 = (C - 1)100 \quad (1)$$

where C is the change factor, and $\hat{R}_{\mathrm{T,f}}$ and $\hat{R}_{\mathrm{T,b}}$ are the pooled estimate of the T-year rainfall intensity quantile for the 24-h rainfall duration obtained from future simulations (for a given RCP – horizon combination) and baseline simulations, respectively, for a particular climate model. Relative changes associated with each of the four RCP – horizon combinations are gathered over climate models to form the corresponding ensemble of relative changes (i.e., that associated with RCP 4.5 – 2050, RCP 4.5 – 2080, RCP 8.5 – 2050, and RCP 8.5 – 2080). Multi-model median, lower and upper bounds are then estimated from each ensemble. Multi-model median (i.e., 50$^{\mathrm{th}}$ percentile) indicates the most likely relative change. Multi-model lower bound, defined as 10$^{\mathrm{th}}$ percentile, represents a less likely but possible lower relative change; and multi-model upper bound, defined as 90$^{\mathrm{th}}$ percentile, represents a less likely but possible greater relative change. Multi-model minimum and maximum relative changes are not considered to avoid the most extreme results from the climate models. Multi-model percentile relative changes are computed from ensembles of relative changes (e.g., Sunyer et al. 2015) and not from ensembles of baseline and future quantiles for a more precise estimation.

Climate model simulations present uncertainty, and so does the use of an ensemble of climate models and the estimation of rainfall intensity quantiles. As a result, relative changes may benefit from adjustments for their use in practice. First, coherence in relative changes over horizons for a specific RCP needs to be ensured for the application of relative changes in practice. This is motivated by the necessity of providing design rainfall intensity quantiles that

increase (or stay the same) for later horizons to guarantee reliability. For instance, the relative change factors are expected to be a non-decreasing function of the time horizon considered. In the present study, this is solved by a simple adjustment through which, for a specific RCP, the relative change for both horizons is compared and that associated with 2080 is set equal to the value for the larger of the two relative changes. Coherence in relative changes over RCPs for a specific horizon is, however, not sought since although a higher RCP is expected to lead to a greater global temperature increase, this may not result in larger increasing rainfall intensity at a given location. In this line, Herath et al. (2016) remarked that the Clausius-Clapeyron scaling relationship that links extreme rainfall and temperature may not be valid for high temperatures, for which extreme rainfall may decrease. This could result in the estimation of lower extreme rainfall relative changes for future horizons. Wang et al. (2017) presented evidence of a negative relationship between daily extreme precipitation and temperature for high temperatures across the globe, and underlined that the Clausius-Clapeyron scaling relationship is only valid under constant relative humidity or without moisture limitation. Roderick et al. (2019) pointed out that, in the tropics, negative scaling may be attributed to temperature limitation because of evaporation. For high temperature, the latter may lead to a negative relationship between temperature and integrated water vapor, and hence to lower extreme rainfall as a result of the positive relationship between integrated water vapor and rainfall intensity.

It may be relevant to analyse, and if possible to improve, the agreement in the relationship between relative change and return period over RCP – horizon combinations. One reason is that a decreasing relationship could lead to conflicts when updating rainfall intensity quantiles using relative changes associated with different return periods. To understand this relationship, a linear

regression model between relative change (response) and return period (predictor) is fitted and the corresponding slope (regression coefficient) is estimated at each grid.

3. Case study and data

The case study is Canada (Fig. 1a) and the analysis is based on available NA-CORDEX baseline and future simulations for the study area. NA-CORDEX uses multiple GCMs from the Coupled Model Intercomparison Project Phase 5 (CMIP5) as RCM boundary conditions, in a similar way that the well-known North American Regional Climate Change Assessment Program (NARCCAP) used GCMs from the multiple Coupled Model Intercomparison Project Phase 3 (CMIP3). NA-CORDEX (https://na-cordex.org) aims at supplying simulations for six RCMs driven by six GCMs at several spatial resolutions, considering different RCPs. Bias corrected simulations based on kernel density distribution mapping, planned to be provided by NA-CORDEX, were not available at the time the present study was performed. NA-CORDEX is in progress with several model combinations currently available. NA-CORDEX simulations have been used in recent research (e.g., DeGaetano et al. 2017; Wong et al. 2017; Ganguli and Coulibaly 2019).

The NA-CORDEX data archive is in line with recommendations for estimating projected changes by taking into account different sources of uncertainty, such as by considering several RCMs driven by several GCMs, and different future scenarios. Distinguishing between RCPs avoids merging model uncertainty and human choice uncertainty. Simulations with a similar horizontal resolution and at a common reference grid are also provided. At the time the present study was conducted, six NA-CORDEX model combinations were available according to these criteria and are used herein. The models presented daily temporal resolution, and a spatial resolution of 0.44˚ (~ 50 km) native rotated-pole grid interpolated to a common 0.5˚ latitude-

longitude grid; they presented projections for two RCPs (RCP 4.5 and RCP 8.5) (Mearns et al. 2017). Their nomenclature is established here by first indicating the RCM and then the driving GCM (Table 1): CanRCM4/CanESM2, CRCM5-UQAM/CanESM2, CRCM5-UQAM/MPI-ESM-LR, HIRHAM5/EC-EARTH, RCA4/CanESM2 and RCA4/EC-EARTH. Information about the models may be found at https://na-cordex.org.

NA-CORDEX simulations are available for historical (1950 to 2005) and future (2006 to 2100) periods. The use of a 30-year study period is recommended for climate change assessment and hence, the commonly used baseline period 1971-2000, and future periods 2041-2070 and 2071-2100 are selected in this analysis (e.g., Charron 2014). These future periods are commonly known as horizon 2050 and 2080, and are used in many studies (e.g., Nguyen et al. 2007; Kuo et al. 2015; Herath et al. 2016). A total of 30 grid-scale daily precipitation simulations are used in this study, which comprises five simulations (one baseline simulation and four future simulations) for each of the six NA-CORDEX model combinations (Table 1). Future simulations are associated with each of the four RCP – horizon combinations: RCP 4.5 – 2050, RCP 4.5 – 2080, RCP 8.5 – 2050 and RCP 8.5 – 2080. The NA-CORDEX grid domain used is restricted to Canada, with an upper limit at 65˚ latitude (Fig. 1a). This delimitation is coherent with the domain used when performing pooled frequency analysis based on observed rainfall series (Requena et al. 2019). The use of an upper limit to latitude is also supported by the predominant underestimation of daily precipitation of gridded climate products in northern Canada (Wong et al. 2017).

The pooled estimate of the T-year rainfall intensity quantiles obtained from observed 24-h rainfall in Requena et al. (2019), with return period T = 2, 5, 10, 25, 50 and 100 years, are the observation-based quantiles used in the present study (see Section 2.2 for details about the

pooled approach). The raw data used for estimating these observation-based quantiles consisted of 24-h annual maximum rainfall depth series from 554 of the 565 rainfall stations used by Environment and Climate Change Canada (ECCC) for estimating at-site IDFs (ECCC 2018). The set of 554 stations was obtained by removing six stations north of 65˚ latitude, three stations due to nonstationarity issues and two stations without records for the 24-h rainfall duration. Station location is shown in Section 4.2.

4. Application to Canada

4.1. Extraction of annual maximum rainfall series from grid-scale daily precipitation

Most of the rainfall stations used for IDF estimation in Canada are out of service during the winter months (Hogg et al. 1989). The dataset used in this study for analysing starting and ending months of observed rainfall consisted of 1-h rainfall intensity observed dates from 1937 to 2018 associated with around 18 700 station-years that were provided by ECCC upon request. Three types of classifications are assessed for dividing the country to identify the approach that provides the best representation of rainfall periods: administrative units (e.g., Fig. 1a), ecozones and ecoprovinces (Fig. 1b). Canada consists of 13 administrative units (specifically, 10 provinces and 3 territories), and is divided into 15 ecozones comprising 53 ecoprovinces (Ecological Stratification Working Group (ESWG) 1995; http://sis.agr.gc.ca/cansis/nsdb/ecostrat/index.html).

Three main rainfall period categories are identified across Canada following Section 2.1: January – December (Jan – Dec), March – December (Mar – Dec), and April – November (Apr – Nov). The largest variability is generally associated with the starting month of the first category regardless of the classification considered (i.e., administrative units, ecozones or ecoprovinces).

The classification based on ecoprovinces is selected because it allows for a better characterization of the rainfall period categories across the country thanks to its greater number of subdivisions (Fig. 1). The study domain consists of 4792 grids (Fig. 1a) of which 11.5% are linked to the rainfall category Jan – Dec, 16.5% to Mar – Dec, and 72% to Apr – Nov. The category Jan – Dec is associated with the West Coast, southwestern British Columbia (BC), the southernmost part of Ontario (ON), most of Newfoundland and Labrador (NL) and most of the Maritimes (i.e., Nova Scotia (NS), Prince Edward Island (PE), and part of New Brunswick (NB)). The category Mar – Dec is associated with the rest of BC except its northern part, southern Alberta (AB), southern Saskatchewan (SK), southwestern and southeastern ON, Saint Lawrence River proximities, eastern Quebec (QC), and eastern NL. The category Apr – Nov is associated with the rest of the country.

Grid-scale daily annual maximum rainfall series are extracted from grid-scale daily precipitation simulations using the rainfall period category associated with each gridpoint. For instance, for a grid associated with the rainfall period category Apr – Nov, this means that the daily annual maximum rainfall at the grid is the maximum value associated with rainfall occurring from April to November (i.e., without considering rainfall that occurred in January, February, March or December). This is done for the 30 NA-CORDEX simulations. The use of the three rainfall period categories to extract annual maximum series at grids belonging to each type of category is briefly analysed for discussion. Annual maximum series extracted at grids belonging to the categories Mar – Dec and Apr – Nov are found to be less affected by the rainfall period considered. This is likely due to annual maxima generally occurring within the months associated with each category. Annual maximum series extracted at grids belonging to the category Jan – Dec are found to be more affected by the use of shorter periods, which supports

annual maxima occurring throughout the year. Therefore, if it was not possible to assign rainfall period categories for annual maximum rainfall extraction, the use of the entire year (e.g., Mailhot et al. 2012) would be preferred to the use of a shorter period for the entire country (e.g., Mladjic et al. 2011).

Trends on the extracted annual maximum rainfall series are analysed using the block bootstrap Mann-Kendall test, which accounts for serial correlation (Khaliq et al. 2009; Önöz and Bayazit 2012; Sarhadi and Soulis 2017). Significant trends at a 5% significance level are found at fewer than 8.6% of the grids for each simulation. On average, 5.6% of the grids presented significant trends over the 30 simulations. These percentages are similar to those obtained by Maihot et al. (2012), and analogously, all simulations are assumed as stationary for the purpose of the present study. In this regard, Mailhot et al. (2007) underlined that significant trends may not be identified in commonly used record lengths for studying climate change, even in simulations for future study periods.

4.2. Pooled quantile estimation for grid-scale annual maximum rainfall intensity

An overview of the pooling group characteristics obtained after applying the pooling approach (Section 2.2) to the 30 NA-CORDEX simulations is presented below. The median number of grids in a pooling group ranged from five to 17, depending on the return period. The 25^{th} – 75^{th} percentile interval of the heterogeneity measure H reached up to (-2.3, 0.2) for $T = 100$ years. This is lower than for observations, since grid-scale simulations from climate models are generally more correlated (Li et al. 2017). Maximum distance from grids in a pooling group to the target grid was less than 290 km.

Grid-scale pooled estimates of the T-year rainfall intensity quantile for the 24-h rainfall duration are obtained using the generalized extreme value distribution, which is recommended as

the pooled parent distribution in Canada (Requena et al. 2019). Daily annual maximum rainfall intensity series from NA-CORDEX simulations were multiplied by a factor of 1.13 (World Meteorological Organization (WMO) 2009), to convert daily annual maximum rainfall intensity to 24-h rainfall intensity, following ECCC's practice. A similar factor of 1.15 is used in Australia to obtain 24-h annual maximum rainfall series from daily rainfall observations (Johnson and Green 2018). Papalexiou et al. (2016) indicted that this multiplier, known as Hershfield factor, may be treated as a random variable within [1, 2], for which different values are associated with different exceedance probabilities. When treated as a random variable, the uncertainty introduced may result in larger uncertainty in quantiles estimates. The mean value, commonly used in practice, presents an exceedance probability of around 35% for rainfall durations greater than 6h. The pooled estimate of the *T*-year rainfall intensity quantile for the 24-h rainfall duration, with *T* = 2, 5, 10, 25, 50 and 100 years, is obtained at each grid for each of the 30 NA-CORDEX simulations.

Grids with at least one station are identified for comparison between observation-based and baseline quantiles. Only 388 of the 4792 grids in the study domain contained at least one station, which represents around 8% of the grids. The percentage of grids regarding those with a given number of stations (over all return periods), for which the multi-model median baseline quantile is within the observation-based quantile range, is found to increase as the number of stations increases from two to four stations in a grid (Fig. 2a). The median percentage of grids fulfilling the criterion ranged from 18% to 50%. The increase may be expected, since the presence of a greater number of stations may provide more information about the spatial distribution of rainfall intensity within the grid. Results for grids with more than five stations are not discussed here due to the low number of occurrences of these events (Fig. 2; text within parenthesis below x-axis

ticks). Results for grids with just one station cannot be obtained in this case, since at least two observation-based quantiles are needed to form the assessing range (Fig. 2a).

The analysis of the analogous percentage of grids for which multi-model median baseline quantile is less than the maximum observation-based quantile is computed for comparison purposes (Fig. 2b). This analysis generates results for grids with at least one station. For grids with one to three stations, the percentage of grids fulfilling this latter criterion was larger than that for the previous analysis, whereas both analyses provided similar results for grids with at least four stations. This implies that if a baseline quantile is less than the maximum observation-based quantile at the grid, it is more likely for it to also be within observation-based quantile range when the number of stations within the grid is large. This may be expected, since a greater number of stations provides a better representation of rainfall intensity within the grid and more chances for the baseline quantile to be within the observation-based quantile range. Differences between observation-based and baseline quantiles are also expected since NA-CORDEX simulations are not bias corrected and such comparison is based on quantile estimates rather than on "measured" values. Therefore, the two aforementioned criteria may be considered as reasonableness tests, where false outcomes do not invalidate either type of estimate.

The results for the present case study indicate a better representation of the "areal" versus "point" relationship for grids containing at least four stations. This is in line with the general recommendation of the WMO for the control area of a gauge station to be less than 600 km^2 (Tian et al. 2018), which is equivalent to at least four stations per 2500 km^2. Note that areal reduction factors to deal with differences between point and gridded rainfall intensity are not available for the entire Canada mainly due to the low density of the gauge network (Mailhot et al. 2012). Areal reduction factors may change depending on the region, rainfall duration and

return period (DeNeale et al. 2018), and may be affected by climate change (Li et al. 2015). The results also underline the difficulty in bias correcting grid-scale simulations when gauge density is low, since spatial distribution of observed rainfall intensity may not be reliably estimated for the grid. The assumption in the present study is that bias from climate models affects baseline and future simulations in a similar way and hence the associated relative change (through which computation bias is cancelled out) may be considered as suitable for updating observation-based quantiles (e.g., Ekström et al. 2005). Note that the lack of a dense gauge density in Canada prevents a fair direct comparison of quantiles from RCM simulations and observations, since it is not possible to perform a suitable bias correction of gridded RCM simulations and use areal reduction factors for the entire country.

Spatial distribution of grids under these criteria is displayed in Fig. 3a and Fig. 3b, respectively, for T = 100 years as an illustration. 28% of the 79 grids with at least two stations fulfilled the first criterion for T = 100 years (Fig. 3a), and 42% of the 388 grids with at least one station fulfilled the second criterion for T = 100 years (Fig. 3b). Spatial results indicate that the ensemble of NA-CORDEX model combinations may provide representative relative changes across Canada, since grids for which the baseline quantile is within the observation-based quantile range, or for which the baseline quantile is less than the maximum observation-based quantile, may be found across the country. Similar conclusions apply to other return periods.

4.3. Grid-scale relative change before adjustments

Grid-scale 24-h relative change for RCP – horizon combinations are estimated across Canada as indicated in Section 2.3. Boxplots for RCP 8.5 – 2050 and RCP 8.5 – 2080 are shown in Fig. S1 in the supplementary material as an illustration. Median relative change over return periods increased with RCP and horizon for all multi-model percentiles, following the order RCP

4.5 – 2050, RCP 4.5 – 2080, RCP 8.5 – 2050, RCP 8.5 – 2080. Considering each return period separately, minimum 25th percentile and maximum 75th percentile also kept this order; yet this was not always the case for minimum and maximum relative change. The latter anticipates potential lack of coherence over RCPs or horizons at particular locations. Relative change variability increased with return period for all cases. Median relative change presented a decreasing relationship with return period for multi-model 10th percentile, an increasing relationship for multi-model 90th percentile, and remained constant for multi-model 50th percentile, which stresses the greater relative change variability with return period.

The spatial distribution of grid-scale 24-h relative change is also analysed, and relative changes are extracted at specific locations across Canada to further illustrate the results. Capital cities of Canadian administrative units, and Canada are the locations used for this analysis. For simplicity and comparison with existing studies, the closest station to the geographical coordinates of the city is identified (Table 2), and the associated relative change is considered as that at the grid where the station is located. In practice, the area of the specific city (or the area of a catchment) could be used for identifying associated grids, through which an average relative change may be estimated. The corresponding maximum relative change may be obtained instead, if a design accounting for potential relative changes anywhere within the city (or catchment) is desired. The latter option would be in line with discussion in Bárdossy and Pegram (2018).

Multi-model 50th percentile grid-scale 24-h relative change presented different values and relationships with return period, RCP and horizon across cities, with changes ranging from -11% to 51% when considering the four RCP – horizon combinations (Table 3). All cities presented positive relative changes, except Halifax for RCP 4.5 – 2050, where large negative relative changes are found. The relationship of relative change with return period may change across

RCP – horizon combinations for a city. For instance, Ottawa presented a positive relationship for RCP 4.5 – 2050 but a negative relationship for RCP 4.5 – 2080 (not shown). Different relationships of relative change with return period across horizons may also be seen in other studies (e.g., Herath et al. 2016 Table 4).

Min, mean and max multi-model 50th percentile relative change over return periods at cities increased between 2050 and 2080 (i.e., over horizons) for RCP 8.5, and between RCP 4.5 and RCP 8.5 (i.e., over RCPs) for 2080 (Table 3). The only exception was St. John's, with mean and max relative change for RCP 8.5 – 2080 less than for RCP 8.5 – 2050 (Table 3; bold values in the last two columns). However, many cases presented lack of coherence when looking at relative change over horizons for RCP 4.5, and over RCPs for 2050 (Table 3; bold values from columns two to seven); this underlines a general discrepancy associated with relative changes for RCP 4.5 – 2050. Analysis of relative changes at grids within the entire domain supported the generalization of this finding, although with many exceptions. Overall results are hence in line with behaviour of global surface temperature change (e.g., Charron 2014 Figure 20). That is, a more marked difference among climate models is seen (i) for a later horizon (2080) in comparison with a nearer one (2050) when using a higher RCP (RCP 8.5), and (ii) among RCPs (RCP 4.5 and RCP 8.5) when considering a later horizon (2080). In view of these results and taking into account that a higher RCP may be more likely for the nearer horizon 2050, RCP 4.5 – 2050 is no longer considered in the present study and hence, associated adjustments over horizons are not applied to RCP 4.5 – 2080.

4.4. Grid-scale relative changes after adjustments

The previous results underlined the large variability of multi-model percentile grid-scale 24-h relative changes across Canada and hence, the need for adjustments to provide coherent

relative changes for extreme rainfall intensity update under climate change. The agreement in the relationship between relative change and return period over RCP – horizon combinations is analysed through the estimation of the associated regression slope. Slope magnitude ranged from -0.5 to 1.3, and increased with multi-model percentile (Fig. 4). There was a larger negative slope presence for multi-model 10th percentile, and a larger positive slope presence for multi-model 90th percentile. Slope sign (Fig. 5a) supported these results and showed a relatively high spatial coherence of grids with coherent slope sign over the three retained RCP – horizon combinations.

The slope range [-0.06, 0.06] (i.e., from a decreasing 6% to an increasing 6% slope) is considered to be small enough to characterise a constant relationship between relative change and return period. Relative change for grids with a constant slope is assigned to be the corresponding mean relative change over return periods. This is done for each of the three RCP – horizon combinations. The slope range [-0.06, 0.06] is used as this range results in an absolute maximum difference no greater than 15% for relative changes at return periods before and after the adjustment. As an illustration, the slope magnitude for RCP 8.5 – 2080 is shown in Fig. 5b, indicating grids with slopes within that range. The adjustment aims at improving the agreement in the relationship between relative change and return period over RCP – horizon combinations for application of relative changes in practice. The average percentage of grids affected by this adjustment is 30%, 41% and 17% for the multi-model 10th, 50th and 90th percentile, respectively, when accounting for the three RCP – horizon combinations. Adjustment for coherence over horizons affected an average of 13% of grids for RCP 8.5, when accounting for all multi-model percentiles and return periods. This adjustment would have affected an average of 37% of grids if applied to RCP 4.5. An additional check is done to ensure coherence over multi-model

percentiles after the two previous adjustments. The average percentage of grids affected by this is negligible (about 0.1%).

Boxplots of grid-scale 24-h relative change before (e.g., Fig. S1) and after (not shown) adjustments presented similar overall behaviour. Nevertheless, as expected, after adjustments the analysed statistics stayed the same or increased with horizon for RCP 8.5. A similar median multi-model 50th percentile of 14%, 16% and 27% was obtained before and after adjustments for RCP 4.5 – 2080, RCP 8.5 – 2050, and RCP 8.5 – 2080, respectively, as well as a similar overall range for relative change (-46%, 182%). Multi-model 50th percentile ranged from -17% to 88% when considering the three retained RCP – horizon combinations. As an illustration, grid-scale 24-h relative changes after adjustments for T = 2 and 100 years are shown for RCP 8.5 – 2080 in Fig. 6. Corresponding results for RCP 4.5 – 2080 and RCP 8.5 – 2050 are displayed as Figs. S2 and S3 in the supplementary material. In general, relative changes for RCP – horizon combinations varied smoothly and formed a number of clusters of similar values across the country. Negative relative changes were mostly related to multi-model 10th percentile. Multi-model 90th percentile presented practically no negative relative changes. Multi-model 50th percentile presented few small clusters of negative relative changes. In general, relative changes increased in magnitude with return period.

As expected from adjustments, min, mean and max multi-model 50th percentile 24-h relative change over return periods are equal or increase with horizon for RCP 8.5 at cities (Table 4). In general, relative changes for RCP 4.5 – 2080 are closer to values for RCP 8.5 – 2050, and less than RCP 8.5 – 2080. Adjustments for cities are generally small and related to the use of a constant slope, except for St. John's for RCP 8.5 – 2080, where adjustments due to lack of coherence between horizons were needed. Small and coherent mean multi-model 50th percentile

over return periods for the three RCP – horizon combinations (RCP 4.5 – 280, RCP 8.5 – 2050 and RCP 8.5 – 2080) are found at Halifax (5%, 11% and 20%), Quebec City (10%, 12% and 21%), Victoria (7%, 8% and 16%) and Winnipeg (9%, 8% and 21%). Coherent large values for the three RCP – horizon combinations are found at Edmonton (25%, 24% and 32%), Iqaluit (24%, 24% and 37%) and Whitehorse (31%, 39% and 49%), which are generally located north of the rest of the sites. Positive multi-model 50th percentile relative changes are found at capital cities for the three RCP – horizon combinations (Fig. 7 and Figs. S4 to S6; colored lines).

Multi-model 10th, 50th and 90th percentile grid-scale 24-h relative change after adjustments are presented for Edmonton, Ottawa, Toronto and Victoria as representative of different behaviours in Fig. 7; results for the rest of the cities are displayed in Figs. S4 to S6 in the supplementary material. The associated regression slope between relative change and return period is shown in Table 5. Victoria presented an overall constant relationship of relative change with return period (Fig. 7), with a similar behaviour in Iqaluit (Fig. S4). Edmonton showed an overall positive relationship between relative change and return period (Fig. 7), with a similar behaviour in Fredericton (Fig. S4). Ottawa displayed a positive relationship between relative change and return period for multi-model 90th percentile, and a negative relationship for multi-model 10th percentile (Fig. 7). A similar behaviour is seen in Charlottetown and St. John's (Fig. S4). Toronto presented a mixed behaviour (Fig. 7), as well as the rest of the cities (Figs. S5 and S6). Most cities belonged to this last category.

4.5. Comparison of relative changes with existing studies

Grid-scale 24-h (or daily) relative changes using a fixed-region approach are provided for Canada by two studies: Mailhot et al. (2012) and Mladjic et al. (2011). A web tool is also available to estimate future IDFs under climate change in Canada, using a local approach

(IDF_CC tool: Simonovic et al. 2016; Schardong et al. 2018). Comparison among results from different studies is complex due to the different methodologies (regional or local), extraction of annual maximum series (annually or from a given period of months), spatial resolution (grid or point), type and number of climate models (dynamical or statistical downscaled GCMs; one model or an ensemble), definition of future scenarios (Special Report on Emissions Scenarios SRES A2, or RCPs), horizons (2041-2070 or at least a 50-year future period) and return periods (up to $T = 20$ years or longer).

Overall comparison among approaches is done by extracting relative changes (if available) for $T = 2$ and 100 years at the location of the stations associated with each city (Table 2). An overview of the outcome is presented below; further results and discussion are shown in the supplementary material (text and Fig. S7). Relative changes for $T = 2$ years presented positive values for all cities and a similar range for all compared approaches. In general, positive relative changes were also found for $T = 100$ years, but the overall range of relative changes over cities differed among approaches. The lowest range is associated with Mladjic et al. (2011), whereas the largest range is associated with the IDF_CC tool. Larger overall values obtained by the IDF_CC tool could be related to the longer future period (2041-2100) used, the estimation of point- instead of grid-scale rainfall intensity, the different type of climate models considered, and the use of a local approach. Lower overall values associated with Mladjic et al. (2011) could be related to the use of a single RCM, and the use of the period April to September for annual maximum series extraction for all of Canada. As expected, the estimation of relative changes at a particular location depended on the approach. The smallest differences between relative changes from the IDF_CC tool and the present study, considering both return period values and RCPs,

are found for Charlottetown, St. John's and Yellowknife. The largest differences are found for Halifax and Iqaluit.

5. Discussion

Estimation of relative changes in 24-h extreme rainfall intensity is dependent on the climate model simulations used. Additional model combinations may avoid more extreme relative changes when computing multi-model percentiles. Therefore, current relative changes should be updated as additional simulations from NA-CORDEX model combinations become available. Up to 36 NA-CORDEX model combinations are expected. Higher resolution (0.22˚ ~ 25km) grid-scale relative changes could be provided when associated NA-CORDEX simulations are accessible for several RCPs. However, a lack of grid resolution influence on relative change was found when performing an upscaling experiment using NA-CORDEX simulations for the State of New York (DeGaetano et al. 2017).

Regional approaches do not usually consider temporal downscaling and hence, the temporal resolution of the estimated relative changes is at most that given by the temporal resolution of the climate model (e.g., Mailhot et al. 2007). Future research will deal with the estimation of grid-scale relative changes for sub-daily rainfall durations to allow for a complete IDF update. The application of relative changes in practice needs to lead to physically possible IDFs. This may only be ensured for increasing relative change with return period and decreasing relative change with duration, which implies that joint adjustments may be needed in practice.

Low gauge density is problematic for obtaining accurate gridded products for an entire country, such as in the case of Canada (e.g., Roy et al. 2017; Wong et al. 2017). This premise is also supported by the analysis of baseline and observation-based quantiles performed in this

study as a function of the number of stations in a grid. In this line, Tian et al. (2018) found dependence of the performance of a (grid-scale) satellite-based rainfall product on gauge density in China, with higher gauge density improving values of assessment metrics. Thus, bias correction of grid-scale simulations using observations of a similar resolution is not performed in the present study. The application of the alternative scale-adapted statistical bias correction approach (Haerter et al. 2015), where grid-scale simulations may be bias corrected by station-scale observations through data aggregation, is not possible due to the limited available temporal resolution for simulations. The estimation of relative changes is hence based on the delta change method.

Further research may be conducted to estimate grid-scale 24-h relative changes in areas of Canada where a denser gauge network is available and hence, where grid-scale observations may be more accurate. This could allow for a more precise relative change estimation in these areas, since bias correction may reduce change magnitude (Li et al. 2017). Recently, the IDF_CC tool incorporated the estimation of grid-scale IDFs for Canada with the aim of providing future IDFs at ungauged locations using the delta change method, under a local quantile estimation approach (Schardong et al. 2018). Grid-scale annual maximum series used for obtaining those IDFs were estimated from grid-scale reanalysis predictors, and machine learning models calibrated at the closest station. Spatial correction factors at the station were also considered. The performance of the procedure is therefore expected to be affected by station density.

Positive multi-model 50th percentile grid-scale relative changes generally obtained over Canada by the present study support the need of considering the effect of climate change on 24-h extreme rainfall intensity in the country. This effect is not uniform and hence, needs to be assessed for the area of interest. Since the estimation of relative changes is dependent on the

climate model simulations considered, additional models should be incorporated when available to account for as much information as possible in their estimation. Grid-scale 24-h relative changes estimated in the present study may be applied to update 24-h observation-based rainfall intensity quantiles available at a particular location, catchment or city across the country. Multi-model 50th percentile relative change may be seen as the most likely relative change; however, variability in relative changes should be accounted for in practice by also considering the potential effect of multi-model bounds. For safety, it is not recommended to apply negative relative changes to update rainfall intensity quantiles in practice.

6. Conclusions

A methodology for obtaining grid-scale relative changes based on pooled rainfall intensity quantiles estimated from baseline and future climate model simulations is proposed in the present study. The pooled approach allows for a more accurate estimation of quantiles for longer return periods. The methodology is applied to Canada, where six NA-CORDEX model combinations at a common 0.5˚ latitude-longitude grid are used to generate multi-model 10th, 50th and 90th percentile grid-scale 24-h relative changes for six return periods up to 100 years.

Grid-scale 24-h relative changes are estimated for two future scenarios, RCP 4.5 and RCP 8.5, and two horizons, 2050 and 2080. Analysis of the relationship between relative change and return period is performed, and adjustments are done when this relationship may be considered as constant to facilitate the application of relative changes in practice. As a result of analysing coherence of relative changes over horizons, relative changes for RCP 8.5 are recommended for 2050, whereas either relative changes for RCP 4.5 or RCP 8.5 could be used for 2080.

In general, relative changes varied smoothly and formed a number of clusters of similar values across the country. Multi-model 50th percentile relative change were mostly positive,

with a few small clusters of negative values and ranged from -17% to 88%, with a median of 14%, 16% and 27% for RCP 4.5 – 2080, RCP 8.5 – 2050, and RCP 8.5 – 2080, respectively. Relative changes provided for capital cities, as those associated with the grid where the closest station is located, revealed positive multi-model 50th percentile for the three RCP – horizon combinations, and different behaviours of multi-model percentiles as a function of return period. Comparison with existing studies using different approaches and climate models showed an overall agreement in estimating positive multi-model median (or mean) relative changes at the selected cities, whereas different values were assigned to each particular city depending on the approach. A more marked difference in the range of relative changes over cities among approaches was found for a longer return period.

Acknowledgements

This work was supported by the Natural Sciences and Engineering Research Council of Canada (NSERC) under Grant NETGP-451456, Canadian FloodNet. The authors thank Ka-Hing Yau from the Engineering Climate Service Unit of ECCC for suppling starting and ending dates of 1-h rainfall intensity at stations in Canada, as well as to Seth McGinnis from NA-CORDEX for communications about data availability. The assistance from Zhe Yang in providing the base code for automatically downscaling NA-CORDEX simulations, and from Tania Gill in extracting the data needed from existing studies for comparison of relative changes, is also acknowledged. The authors thank Simon Michael Papalexiou and one anonymous reviewer for their critical comments, which helped improve the quality of the manuscript.

The present study was developed under the free software environment R (R Core Team 2018). The authors would like to thank the authors of the packages used: *boot* (Canty and Ripley 2017), *doparallel* (Microsoft Corporation and Weston 2017b), *downloader* (Chang 2015),

foreach (Microsoft Corporation and Weston 2017a), *geosphere* (Hijmans 2017), *httr* (Wickham 2017), *Kendall* (McLeod 2011), *lmomRFA* (Hosking 2017), *ncdf4* (Pierce 2017), *ncdf4.helpers* (Bronaugh 2014), *rasterVis* (Lamigueiro and Hijmans2018), *RColorBrewer* (Neuwirth 2014), *rgdal* (Bivand et al. 2018), *rgeos* (Bivand and Rundel 2018), *trend* (Pohlert 2018), and *xlsx* (Dragulescu and Arendt 2018).

Acronym list

Acronym	Definition
AB	Alberta
BC	British Columbia
CMIP3	Coupled Model Intercomparison Project Phase 3
CMIP5	Coupled Model Intercomparison Project Phase 5
ECCC	Environment and Climate Change Canada
ESWG	Ecological Stratification Working Group
GCM	Global climate model
IDF	Intensity-duration-frequency
MB	Manitoba
NA-CORDEX	North American Coordinated Regional Climate Downscaling Experiment
NARCCAP	North American Regional Climate Change Assessment Program
NB	New Brunswick
NL	Newfoundland and Labrador
NS	Nova Scotia
NSERC	Natural Science and Engineering Research Council
NT	Northwest Territories
NU	Nunavut
ON	Ontario
PE	Prince Edward Island
QC	Quebec
RCM	Regional climate model
RCP	Representative Concentration Pathways
SRES	Special Report on Emissions Scenarios
SK	Saskatchewan
WMO	World Meteorological Organization
YT	Yukon

References

Bárdossy A and Pegram G. 2018. Intensity–duration–frequency curves exploiting neighbouring extreme precipitation data. Hydrological Sciences Journal 63(11):1593-604.

Bivand R and Rundel C. 2018. rgeos: Interface to geometry engine - open source ('GEOS'). R package version 0.3-28. https://CRAN.R-project.org/package=rgeos.

Bivand R, Keitt T and Rowlingson B. 2018. rgdal: Bindings for the 'geospatial' data abstraction library. R package version 1.3-4. https://CRAN.R-project.org/package=rgdal.

Bronaugh D (for the Pacific Climate Impacts Consortium). 2014. ncdf4.helpers: Helper functions for use with the ncdf4 package. R package version 0.3-3. https://CRAN.R-project.org/package=ncdf4.helpers.

Burn DH. 1990. Evaluation of regional flood frequency analysis with a region of influence approach. Water Resour Res 26(10):2257-65.

Burn DH and Taleghani A. 2013. Estimates of changes in design rainfall values for Canada. Hydrological Processes 27:1590-1599.

Canty A and Ripley B. 2017. boot: Bootstrap R (S-Plus) functions. R package version 1.3-20.

Chang W. 2015. downloader: Download files over HTTP and HTTPS. R package version 0.4. https://CRAN.R-project.org/package=downloader.

Charron I. 2014. A guidebook on climate scenarios: Using climate information to guide adaptation research and decisions. Ouranos, 86 p.

Dalrymple T. 1960. Flood frequency analyses. U.S. Geol. Surv. Water Supply Pap. 1543A: 11–51.

DeGaetano AT and Castellano CM. 2017. Future projections of extreme precipitation intensity-duration-frequency curves for climate adaptation planning in New York State. Climate Services 5:23-35.

DeNeale S, Kao SC, Yegorova E, Kanney J and Carr ML. 2018. A Comparative Evaluation of Precipitation Areal Reduction Factor Variability across the Conterminous United States. In AGU Fall Meeting Abstracts.

Dragulescu AA and Arendt C. 2018. xlsx: Read, write, format Excel 2007 and Excel 97/2000/XP/2003 files. R package version 0.6.1. https://CRAN.R-project.org/package=xlsx.

ECCC. 2018. Engineering climate datasets, intensity-duration-frequency (IDF) files, v2.30 2014-12-21. Available at http://climate.weather.gc.ca/prods_servs/engineering_e.html. Last access January 2018.

Ekström M, Fowler H, Kilsby C and Jones P. 2005. New estimates of future changes in extreme rainfall across the UK using regional climate model integrations. 2. Future estimates and use in impact studies. Journal of Hydrology 300(1-4):234-51.

Ecological Stratification Working Group (ESWG). 1995. A national ecological framework for Canada. Agriculture and Agri-Food Canada, Research Branch, Centre for Land and Biological Resources Research and Environment Canada, State of the Environment Directorate, Ecozone Analysis Branch, Ottawa/Hull. Report and national map at 1:7 500 000 scale.

Fowler H, Ekström M, Kilsby C and Jones P. 2005. New estimates of future changes in extreme rainfall across the UK using regional climate model integrations. 1. assessment of control climate. Journal of Hydrology 300(1-4):212-33.

Ganguli P and Coulibaly P. 2019. Assessment of future changes in intensity-duration-frequency curves for southern Ontario using North American (NA)-CORDEX models with nonstationary methods. Journal of Hydrology: Regional Studies, 22(2019) 100587:2-21.

Haerter JO, Eggert B, Moseley C, Piani C and Berg P. 2015. Statistical precipitation bias correction of gridded model data using point measurements. Geophys Res Lett 42(6):1919-29.

Herath SM, Sarukkalige PR and Nguyen VTV. 2016. A spatial temporal downscaling approach to development of IDF relations for Perth airport region in the context of climate change. Hydrological Sciences Journal 61(11):2061-70.

Hijmans RJ. 2017. geosphere: Spherical trigonometry. R package version 1.5-7. https://CRAN.R-project.org/package=geosphere.

Hogg WD, Carr DA and Routledge B. 1989. Rainfall intensity-duration-frequency values for Canadian locations. Downsview; Ontario; Environment Canada. Atmospheric Environment Service.

Hosking JRM. 2017. Regional frequency analysis using l-moments. R package, version 3.1. URL: https://CRAN.R-project.org/package=lmomRFA.

Hosking JRM and Wallis JR. 1997. Regional frequency analysis: An approach based on l-moments. Cambridge University Press, 240 p.

Johnson F and Green J. 2018. A comprehensive continent-wide regionalisation investigation for daily design rainfall. Journal of Hydrology: Regional Studies 16:67-79.

Khalili M. 2017. An efficient statistical approach to multi-site downscaling of daily precipitation series in the context of climate change. Clim Dyn 49(7-8):2261-78.

Khaliq M, Ouarda TB, Gachon P, Sushama L and St-Hilaire A. 2009. Identification of hydrological trends in the presence of serial and cross correlations: A review of selected methods and their application to annual flow regimes of Canadian rivers. Journal of Hydrology 368(1-4):117-30.

Kotamarthi R, Mearns L, Hayhoe K, Castro CL, and Wuebble D. 2016. Use of climate information for decision-making and impacts research: State of our understanding. Prepared for the Department of Defense, Strategic Environmental Research and Development Program. 55p.

Kuo C, Gan TY and Gizaw M. 2015. Potential impact of climate change on intensity duration frequency curves of central Alberta. Clim Change 130(2):115-29.

Kuo C, Gan TY and Hanrahan JL. 2014. Precipitation frequency analysis based on regional climate simulations in central Alberta. Journal of Hydrology 510:436-46.

Lamigueiro OP and Hijmans R. 2018. rasterVis. R package version 0.45.

Li J, Evans J, Johnson F and Sharma A. 2017. A comparison of methods for estimating climate change impact on design rainfall using a high-resolution RCM. Journal of Hydrology 547:413-27.

Li J, Sharma A, Johnson F and Evans J. 2015. Evaluating the effect of climate change on areal reduction factors using regional climate model projections. Journal of Hydrology 528:419-34.

Mailhot A, Beauregard I, Talbot G, Caya D and Biner S. 2012. Future changes in intense precipitation over Canada assessed from multi-model NARCCAP ensemble simulations. Int J Climatol 32(8):1151-63.

Mailhot A, Duchesne S, Caya D and Talbot G. 2007. Assessment of future change in intensity–duration–frequency (IDF) curves for southern Quebec using the Canadian regional climate model (CRCM). Journal of Hydrology 347(1-2):197-210.

Maraun D. 2016. Bias correcting climate change simulations-a critical review. Current Climate Change Reports 2(4):211-20.

Maraun D. 2013. Bias correction, quantile mapping, and downscaling: Revisiting the inflation issue. J Clim 26(6):2137-43.

McLeod AI. 2011. Kendall: Kendall rank correlation and Mann-Kendall trend test. R package version 2.2. https://CRAN.R-project.org/package=Kendall.

Mearns LO, et al. 2017. The NA-CORDEX dataset, version 1.0. NCAR Climate Data Gateway, Boulder CO, last access December 2018, https://doi.org/10.5065/D6SJ1JCH.

Microsoft Corporation and Weston E. 2017a. foreach: Provides foreach looping construct for R. R package version 1.4.4. https://CRAN.R-project.org/package=foreach.

Microsoft Corporation and Weston E. 2017b. doParallel: Foreach parallel adaptor for the 'parallel' package. R package version 1.0.11. https://CRAN.R-project.org/package=doParallel.

Mladjic B, Sushama L, Khaliq M, Laprise R, Caya D and Roy R. 2011. Canadian RCM projected changes to extreme precipitation characteristics over Canada. J Clim 24(10):2565-84.

Monette A, Sushama L, Khaliq M, Laprise R and Roy R. 2012. Projected changes to precipitation extremes for northeast Canadian watersheds using a multi-RCM ensemble. Journal of Geophysical Research: Atmospheres 117(D13).

Neuwirth E. 2014. RColorBrewer: ColorBrewer palettes. R package version 1.1-2. https://CRAN.R-project.org/package=RColorBrewer.

Nguyen V, Nguyen T and Cung A. 2007. A statistical approach to downscaling of sub-daily extreme rainfall processes for climate-related impact studies in urban areas. Water Science and Technology: Water Supply 7(2):183-92.

Önöz B and Bayazit M. 2012. Block bootstrap for Mann–Kendall trend test of serially dependent data. Hydrol Process 26(23):3552-60.

Papalexiou SM, Dialynas YG and Grimaldi S. 2016. Hershfield factor revisited: Correcting annual maximum precipitation. Journal of Hydrology 542:884-895.

Papalexiou SM and Montanari A. 2019. Global and Regional Increase of Precipitation Extremes under Global Warming. Water Resources Research (in press). doi.org/10.1029/2018WR024067.

Pierce D. 2017. ncdf4: Interface to Unidata netCDF (Version 4 or Earlier) format data files. R package version 1.16. https://CRAN.R-project.org/package=ncdf4.

Pohlert T. 2018. trend: Non-Parametric trend tests and change-point detection. R package version 1.1.1. https://CRAN.R-project.org/package=trend.

R Core Team. 2018. R: A language and environment for statistical computing. R Foundation for Statistical Computing, Vienna, Austria. https://www.R-project.org/.

Requena AI, Burn DH and Coulibaly P. 2019. Pooled frequency analysis for intensity-duration-frequency curve estimation. Hydrological Processes: 1-15. https://doi.org/10.1002/hyp.13456.

Robson A and Reed D. 1999. Statistical procedures for flood frequency estimation. Flood Estimation Handbook, Volume 3. Institute of Hydrology, Wallingford, UK.

Roderick TP, Wasko C and Sharma A. 2019. Atmospheric Moisture Measurements Explain Increases in Tropical Rainfall Extremes. Geophysical Research Letters 46(3):1375-1382.

Roy P, Fournier É and Huard D. 2017. Standardization guidance for weather data. Climate Information and Climate Change Projections. Montreal, Ouranos, 52 p.

Sarhadi A and Soulis ED. 2017. Time-varying extreme rainfall intensity-duration-frequency curves in a changing climate. Geophys Res Lett 44(5):2454-63.

Schardong A, Gaur A, Simonovic SP and Sandink D. 2018. Computerized tool for the development of intensity-duration-frequency curves under a changing climate. Technical Manual v.3. Water Resources Research Report. The University of Western Ontario, Department of Civil and Environmental Engineering, Ontario, Canada. www.idf-cc-uwo.ca. 62p.

Shephard MW, Mekis E, Morris RJ, Feng Y, Zhang X, Kilcup K and Fleetwood R. 2014. Trends in Canadian short-duration extreme rainfall: Including an intensity–duration–frequency perspective. Atmosphere-Ocean 52:398-417.

Simonovic SP, Schardong A, Sandink D and Srivastav R. 2016. A web-based tool for the development of intensity duration frequency curves under changing climate. Environmental Modelling & Software 81:136-53.

Sunyer MA, Gregersen IB, Rosbjerg D, Madsen H, Luchner J and Arnbjerg-Nielsen K. 2015. Comparison of different statistical downscaling methods to estimate changes in hourly extreme precipitation using RCM projections from ENSEMBLES. Int J Climatol 35(9):2528-39.

Switzman H, Razavi T, Traore S, Coulibaly P, Burn DH, Henderson J, Fausto E and Ness R. 2017. Variability of future extreme rainfall statistics: Comparison of multiple IDF projections. J Hydrol Eng 22(10):04017046.

Tian F, Shiyu H, Long Y, Hongchang H and Aizhong H. 2018. How does the evaluation of the GPM IMERG rainfall product depend on gauge density and rainfall intensity? Journal of Hydrometeorology 19(2):339-349.

Wang G, Wang D, Trenberth KE, Erfanian A, Yu M, Bosilovich MG and Parr DT. 2017. The peak structure and future changes of the relationships between extreme precipitation and temperature. Nature Climate Change 7(4):268.

Wickham H. 2017. httr: Tools for working with URLs and HTTP. R package version 1.3.1. https://CRAN.R-project.org/package=httr.

Willems P, Arnbjerg-Nielsen K, Olsson J and Nguyen V. 2012. Climate change impact assessment on urban rainfall extremes and urban drainage: Methods and shortcomings. Atmos Res 103:106-18.

Wong JS, Razavi S, Bonsal BR, Wheater HS and Asong ZE. 2017. Inter-comparison of daily precipitation products for large-scale hydro-climatic applications over Canada. Hydrology and Earth System Sciences 21(4):2163-85.

World Meteorological Organization (WMO). 2009. Manual on estimation of probable maximum precipitation (PMP). World meteorological organization.

Zhu J, Stone MC and Forsee W. 2012. Analysis of potential impacts of climate change on intensity–duration–frequency (IDF) relationships for six regions in the united states. Journal of Water and Climate Change 3(3):185-96.

Table 1. Six NA-CORDEX model combinations with five grid-scale daily precipitation simulations used in the study.

NA-CORDEX model combination	RCM	GCM	Type of simulation: study period (horizon)
1	CanRCM4	CanESM2	Baseline: 1971-2000; Future for RCP 4.5: 2041-2070 (2050); Future for RCP 4.5: 2071-2100 (2080); Future for RCP 8.5: 2041-2070 (2050); Future for RCP 8.5: 2071-2100 (2080).
2	CRCM5-UQAM	CanESM2	
3	CRCM5-UQAM	MPI-ESM-LR	
4	HIRHAM5	EC-EARTH	
5	RCA4	CanESM2	
6	RCA4	EC-EARTH	

Table 2. Canadian capital cities and closest station. The grid selected for each city is that where the corresponding station is located.

City	Administrative unit	IDF station code	Lon (˚)	Lat (˚)	Rainfall category
Charlottetown	Prince Edward Island (PE)	8300300	-63.13	46.29	Jan – Dec
Edmonton	Alberta (AB)	3012208	-113.52	53.57	Mar – Dec
Fredericton	New Brunswick (NB)	8101605	-66.61	45.92	Jan – Dec
Halifax	Nova Scotia (NS)	8202200	-63.57	44.65	Jan – Dec
Iqaluit	Nunavut (NU)	2402590	-68.55	63.75	Apr – Nov
Ottawa	Canada	6105978	-75.72	45.38	Mar – Dec
Quebec City	Quebec (QC)	7016280	-71.22	46.8	Mar – Dec
Regina	Saskatchewan (SK)	4016560	-104.67	50.43	Mar – Dec
St. John's	Newfoundland and Labrador (NL)	8403506	-52.74	47.62	Jan – Dec
Toronto	Ontario (ON)	6158355	-79.4	43.67	Jan – Dec
Victoria	British Columbia (BC)	1018610	-123.33	48.41	Jan – Dec
Whitehorse	Yukon (YT)	2101300	-135.07	60.71	Apr – Nov
Winnipeg	Manitoba (MB)	5023233	-97.1	49.88	Mar – Dec
Yellowknife	Northwest Territories (NT)	2204100	-114.44	62.46	Apr – Nov

January to December (Jan – Dec); March to December (Mar – Dec); April to November (Apr – Nov).

Table 3. Multi-model 50th percentile grid-scale 24-h relative change (%) at cities before adjustments.

City	RCP 4.5						RCP 8.5					
	2050			2080			2050			2080		
	Min	Mean	Max	Min	Mean	Max	Min	Mean	Max	Min	Mean	Max
Charlottetown	**7**	**9**	12	15	16	18	2	7	14	22	30	37
Edmonton	11	20	28	19	25	34	17	24	31	20	32	41
Fredericton	8	**23**	**37**	8	**22**	**32**	11	19	26	21	34	45
Halifax	-11	-5	5	2	5	8	9	11	14	18	20	21
Iqaluit	19	**26**	**30**	19	**24**	**27**	23	24	28	30	37	40
Ottawa	**15**	**26**	**34**	**13**	**18**	**22**	14	17	19	27	30	32
Quebec City	**10**	**13**	**16**	**6**	**10**	**13**	9	12	15	19	21	22
Regina	-1	6	10	7	15	23	13	17	20	26	33	41
St. John's	10	11	12	**8**	11	17	20	30	43	26	**27**	**29**
Toronto	5	**9**	**13**	**0**	**6**	**12**	6	8	11	26	32	38
Victoria	**7**	**9**	**12**	**3**	**7**	**10**	6	8	10	13	16	18
Whitehorse	20	26	33	23	31	44	31	39	48	48	49	51
Winnipeg	2	**11**	**18**	4	**9**	**14**	6	8	10	19	21	26
Yellowknife	**7**	**13**	**20**	**7**	14	22	5	11	15	25	28	32

Min, mean and max values are estimated over return periods.

Bold values for RCP 4.5 – 2050 indicate cases where relative change do not increase between RCP 4.5 and RCP 8.5 for 2050; all relative changes increase between RCP 4.5 and RCP 8.5 for 2080.

Bold values for 2080 indicate cases where relative change do not increase between 2050 and 2080 for the given RCP.

Table 4. Multi-model 50th percentile grid-scale 24-h relative change (%) at cities after adjustments for the three retained RCP – horizon combinations.

City	RCP 4.5						RCP 8.5		
	2080			2050			2080		
	Min	Mean	Max	Min	Mean	Max	Min	Mean	Max
Charlottetown	**16**	16	**16**	2	7	14	22	30	37
Edmonton	19	25	34	17	24	31	20	32	41
Fredericton	8	22	32	11	19	26	21	34	45
Halifax	**5**	5	**5**	**11**	11	**11**	**20**	20	**20**
Iqaluit	**24**	24	**24**	**24**	24	**24**	30	37	40
Ottawa	13	18	22	**17**	17	**17**	**30**	30	**30**
Quebec City	**10**	10	**10**	**12**	12	**12**	**21**	21	**21**
Regina	7	15	23	**17**	17	**17**	**33**	33	**33**
St. John's	**11**	11	**11**	20	30	43	**27**	**33**	**43**
Toronto	0	6	12	**8**	8	**8**	26	32	38
Victoria	3	7	10	**8**	8	**8**	**16**	16	**16**
Whitehorse	23	31	44	31	39	48	**49**	49	**49**
Winnipeg	4	9	14	**8**	8	**8**	19	21	26
Yellowknife	7	14	22	5	11	15	**28**	28	**28**

Min, mean and max values are estimated over return periods.

Bold values indicate different relative change before and after adjustments.

Table 5. Slope of the regression between relative change and return period at cities. Results for multi-model 10th, 50th and 90th percentile.

City	RCP 4.5						RCP 8.5		
	2080			2050			2080		
	10th	50th	90th	10th	50th	90th	10th	50th	90th
Charlottetown	-	r	+	-	-	+	-	+	+
Edmonton	r	+	+	-	+	+	+	+	+
Fredericton	+	+	+	r	+	+	r	+	+
Halifax	-	r	r	-	r	+	-	r	+
Iqaluit	r	r	r	r	r	+	r	-	r (+)
Ottawa	-	-	+	-	r	+	-	r	+
Quebec City	-	r	+	r	r	+	-	r	+
Regina	r	+	+	-	r	+	r	r	+
St. John's	-	r	+	-	+	+	-	r (+)	+
Toronto	-	-	r	-	r	+	-	+	r
Victoria	r	-	r	-	r	r	-	r	r
Whitehorse	-	+	+	r	+	+	-	r	r
Winnipeg	r	+	+	-	r	+	r	+	+
Yellowknife	-	+	+	r	+	+	-	r	+

Results after adjustments are shown within parenthesis if different from the ones before adjustments.

The symbol "r" indicates slope within the range [-0.06, 0.06], "+" indicates slope > 0.06, and "-" indicates slope < -0.06.

Figure captions

Fig. 1. Canada as case study: (a) gridpoints classified by rainfall period category from ecoprovinces (administrative units indicated); and (b) ecoprovince division (thin black lines) within ecozones (colored regions).

Fig. 2. (a) Percentage of grids within each category in the x-axis, for which multi-model median baseline quantile is within observation-based quantile range; and (b) percentage of grids within each category in the x-axis, for which multi-model median baseline quantile is less than maximum observation-based quantile. Categories in the x-axis represent number of stations within a grid. Boxplots represent values over return periods. Boxes corresponds with the 25^{th} -75^{th} percentile interval; whiskers reach up to 1.5 times the interquartile range.

Fig. 3. Spatial distribution for T = 100 years of (a) grids (with at least two stations) under the criterion of multi-model median baseline quantile within observation-based quantile range; and (b) grids (with at least one station) under the criterion of multi-model median baseline quantile less than maximum observation-based quantile. Points represent stations.

Fig. 4. Slope between grid-scale 24-h relative change and return period. Boxplots for the three retained RCP – horizon combinations in respect of multi-model 10th, 50th and 90th percentile. Boxes corresponds with the 25^{th} -75^{th} percentile interval; whiskers reach up to 1.5 times the interquartile range.

Fig. 5. Slope between grid-scale 24-h relative change and return period: (a) slope sign of grids with coherent slope sign over the three retained RCP – horizon combinations; and (b) slope magnitude for RCP 8.5 – 2080. Multi-model 10th, 50th and 90th percentile results by rows. Grids associated with cities in Table 2 are marked in purple.

Fig. 6. Grid-scale 24-h relative change (%) for RCP 8.5 – 2080 after adjustments. Multi-model 10th, 50th and 90th percentile results (rows) for T = 2 and 100 years (columns). Grids associated with cities in Table 2 are marked in purple.

Fig. 7. Grid-scale 24-h relative change (%) for Edmonton, Ottawa, Toronto and Victoria. Results for RCP 4.5 and RCP 8.5, horizon 2050 (dashed line) and 2080 (continuous line), and multi-model 10th (black), 50th (colored) and 90th (black) percentile. Results for the grid associated with each city (see Table 2).

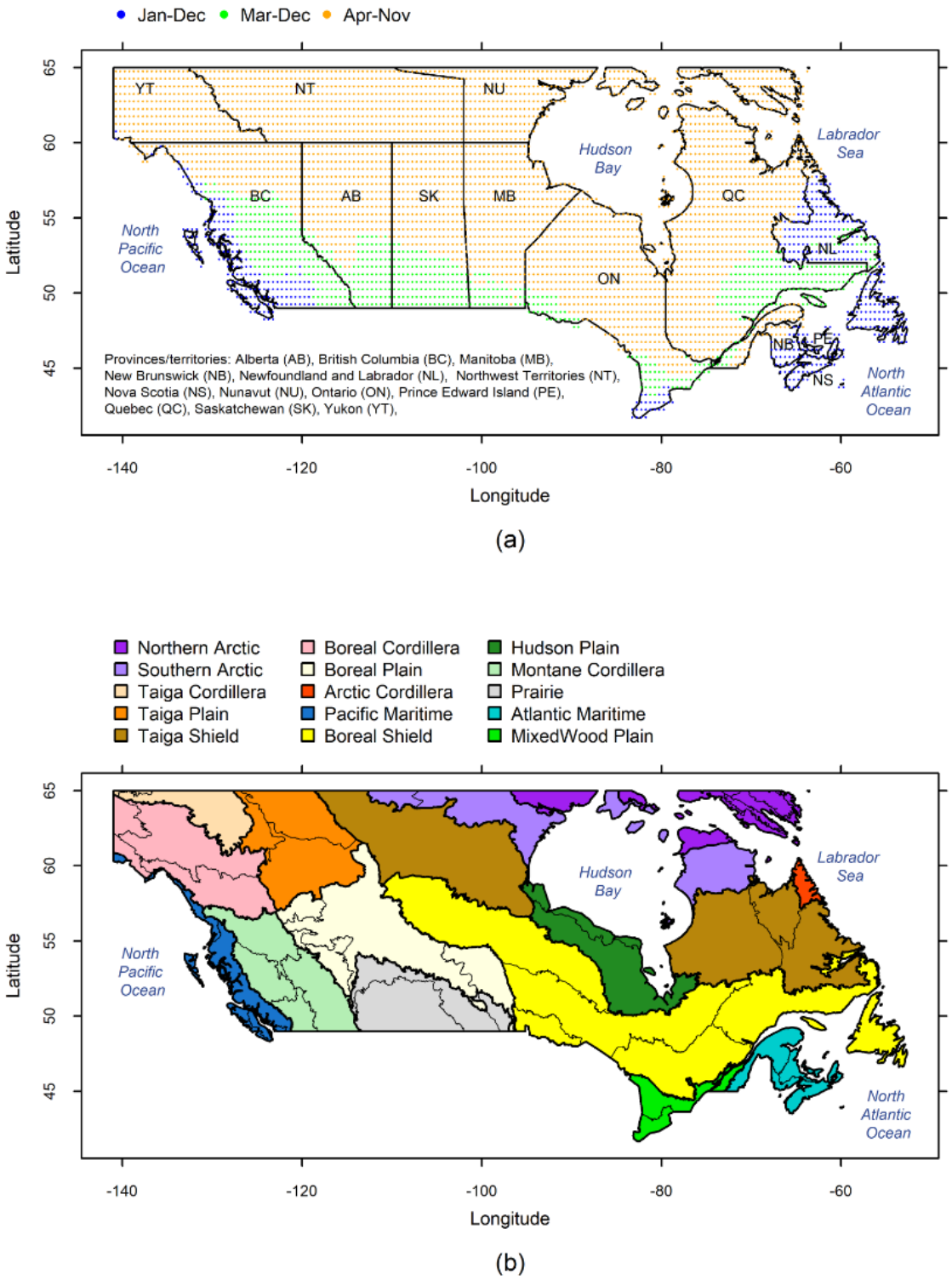

Fig. 1. Canada as study case: (a) gridpoints classified by rainfall period category from ecoprovinces (administrative units indicated); and (b) ecoprovince division (thin black lines) within ecozones (colored regions).

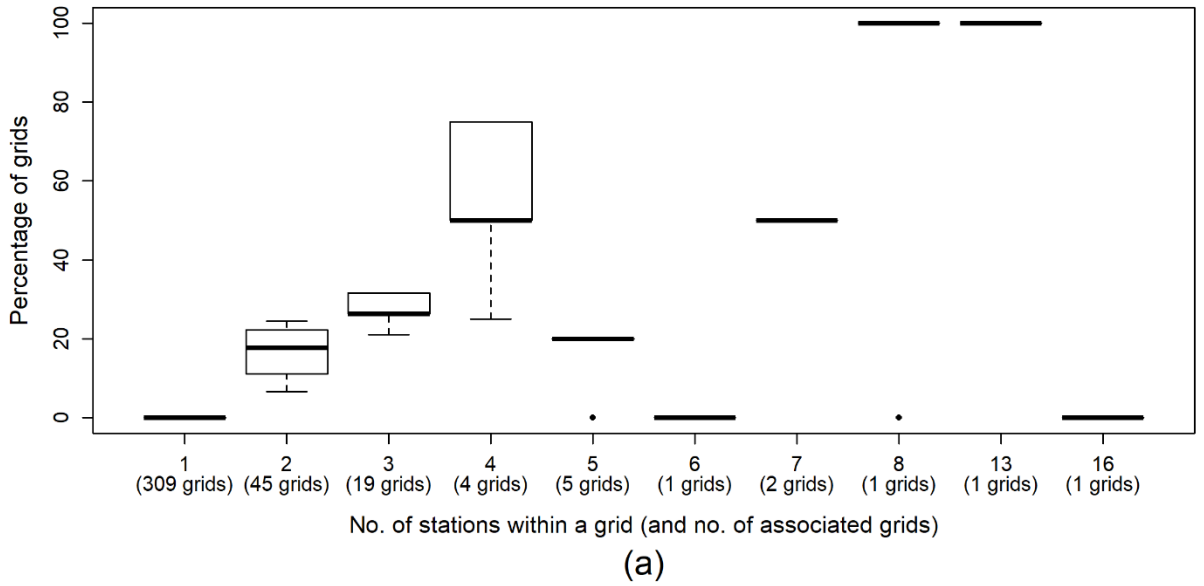

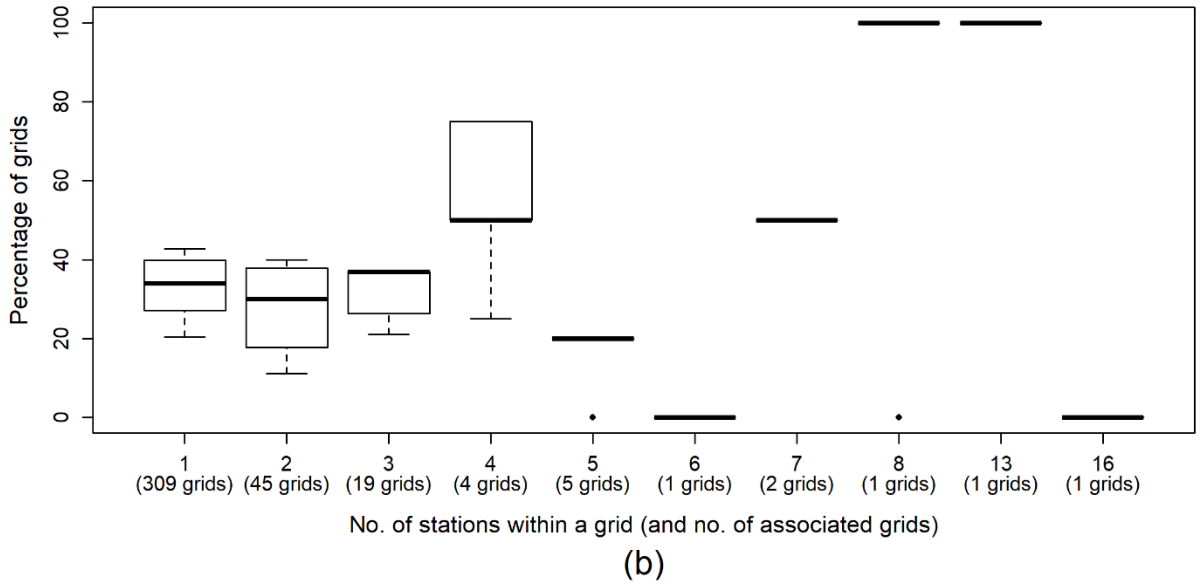

Fig. 2. (a) Percentage of grids within each category in the x-axis, for which multi-model median baseline quantile is within observation-based quantile range; and (b) percentage of grids within each category in the x-axis, for which multi-model median baseline quantile is less than maximum observation-based quantile. Categories in the x-axis represent number of stations within a grid. Boxplots represent values over return periods. Boxes corresponds with the 25th - 75th percentile interval; whiskers reach up to 1.5 times the interquartile range.

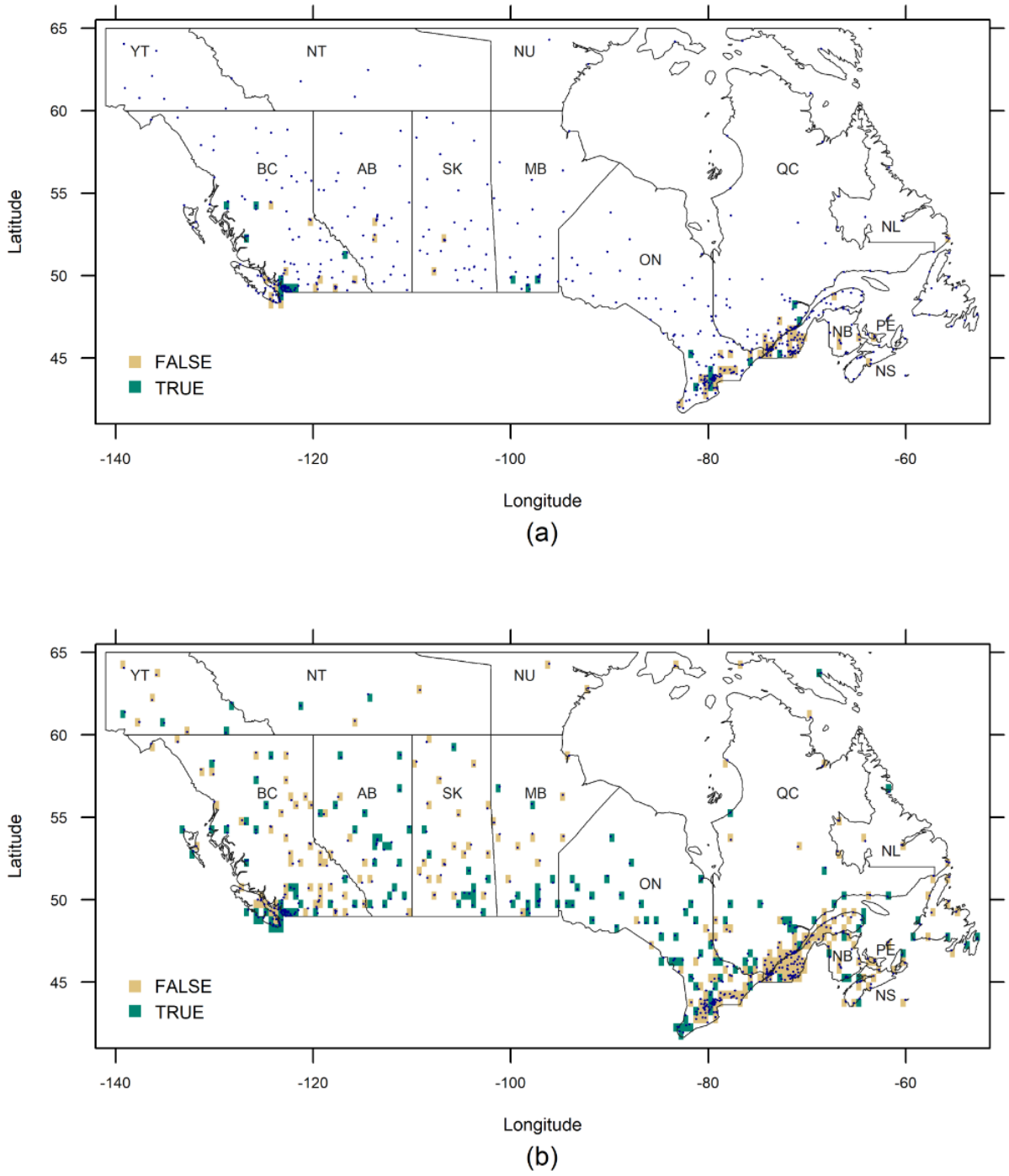

Fig. 3. Spatial distribution for $T = 100$ years of (a) grids (with at least two stations) under the criterion of multi-model median baseline quantile within observation-based quantile range; and (b) grids (with at least one station) under the criterion of multi-model median baseline quantile less than maximum observation-based quantile. Points represent stations.

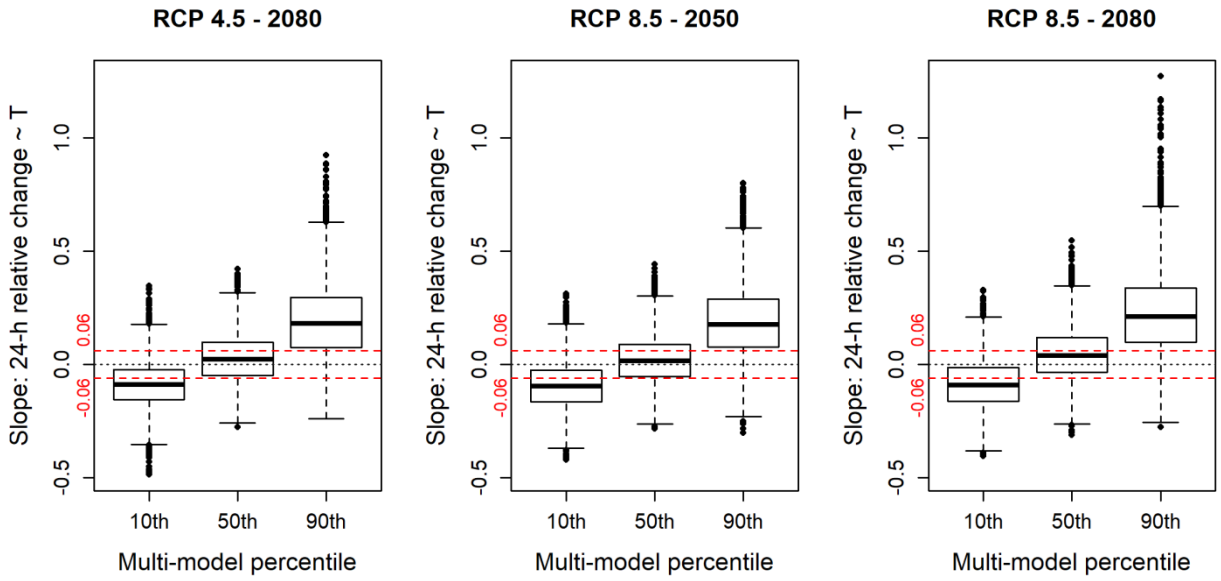

Fig. 4. Slope between grid-scale 24-h relative change and return period. Boxplots for the three retained RCP – horizon combinations in respect of multi-model 10th, 50th and 90th percentile. Boxes corresponds with the 25th -75th percentile interval; whiskers reach up to 1.5 times the interquartile range.

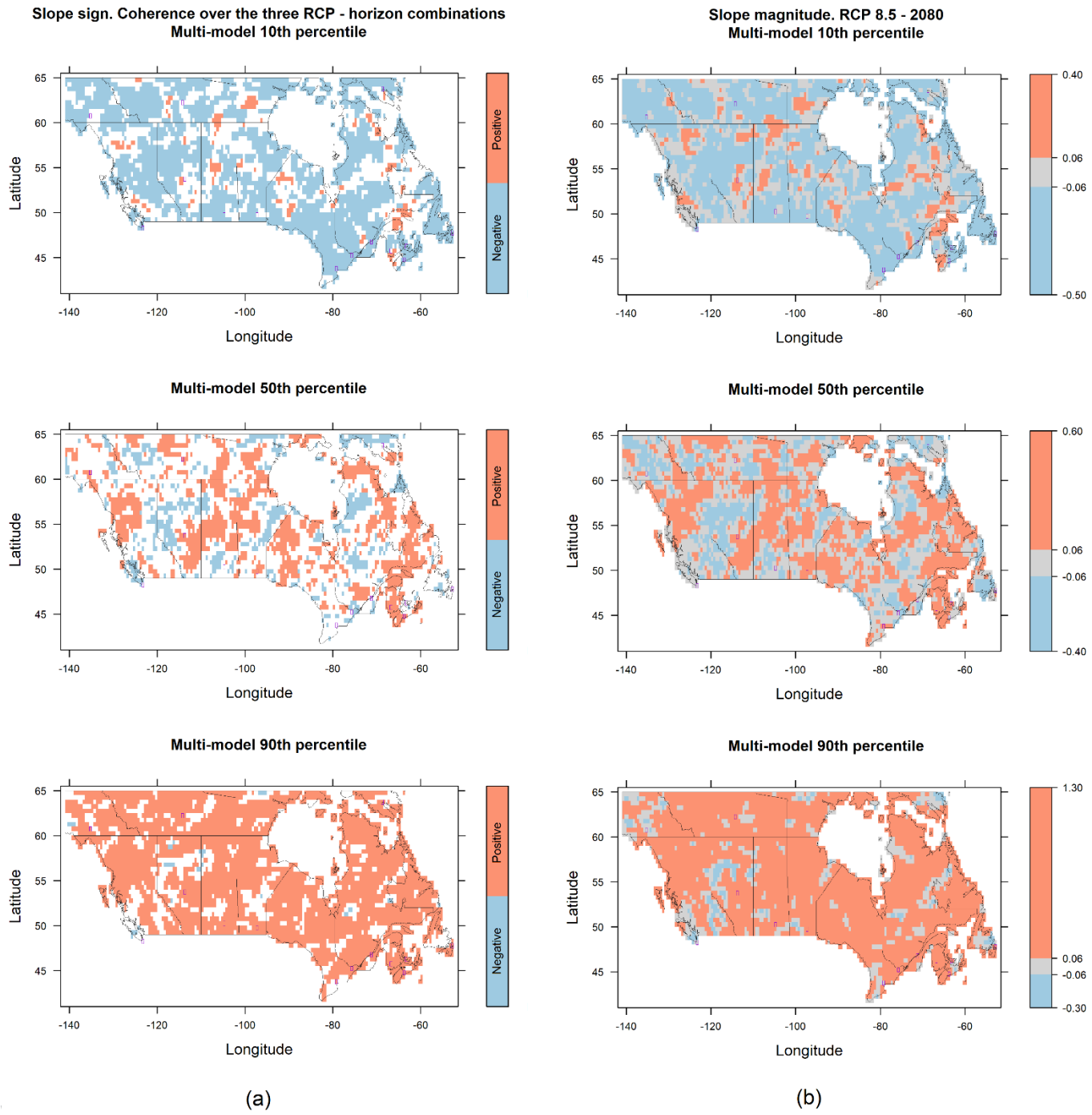

Fig. 5. Slope between grid-scale 24-h relative change and return period: (a) slope sign of grids with coherent slope sign over the three retained RCP – horizon combinations; and (b) slope magnitude for RCP 8.5 – 2080. Multi-model 10th, 50th and 90th percentile results by rows. Grids associated with cities in Table 2 are marked in purple.

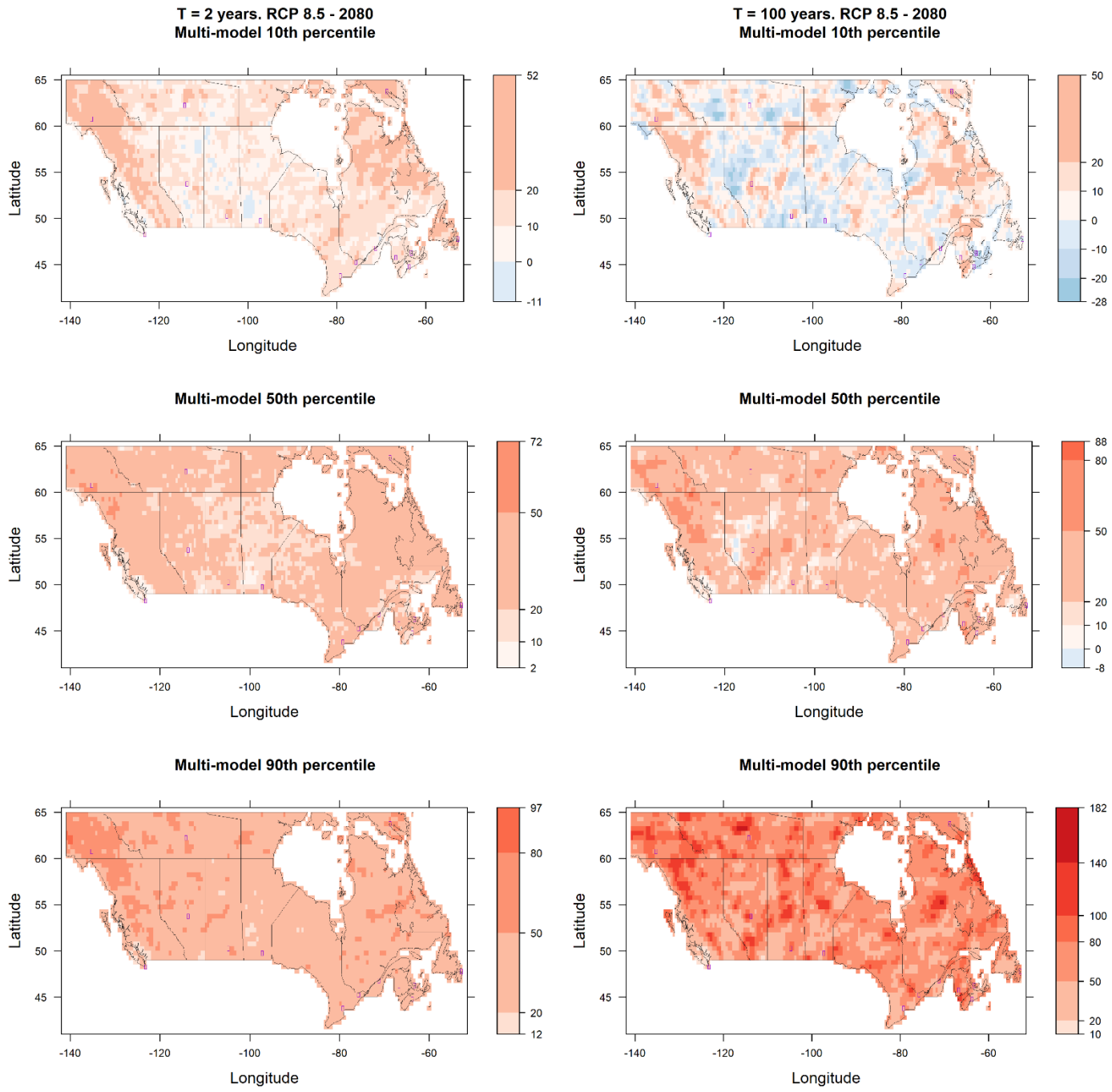

Fig. 6. Grid-scale 24-h relative change (%) for RCP 8.5 – 2080 after adjustments. Multi-model 10th, 50th and 90th percentile results (rows) for T = 2 and 100 years (columns). Grids associated with cities in Table 2 are marked in purple.

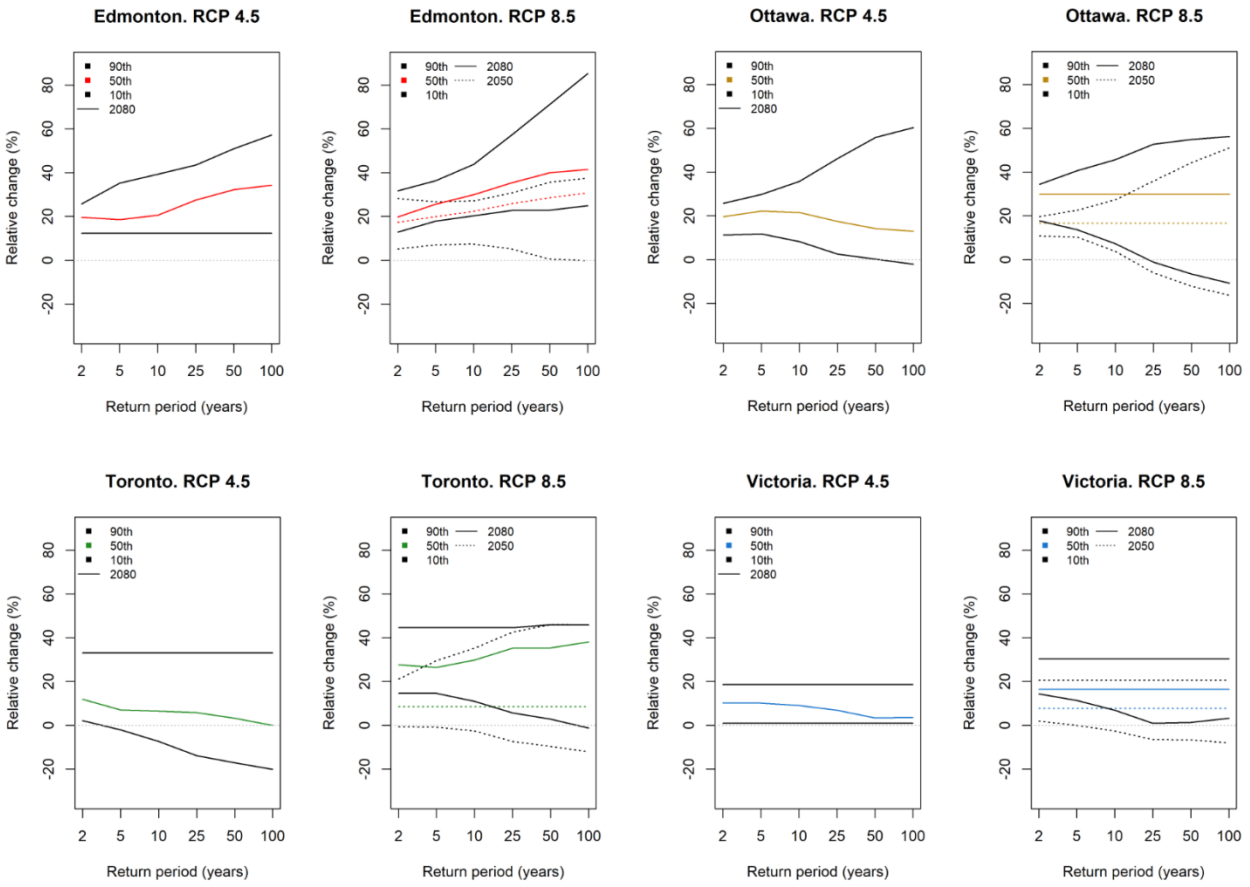

Fig. 7. Grid-scale 24-h relative change (%) for Edmonton, Ottawa, Toronto and Victoria. Results for RCP 4.5 and RCP 8.5, horizon 2050 (dashed line) and 2080 (continuous line), and multi-model 10th (black), 50th (colored) and 90th (black) percentile. Results for the grid associated with each city (see Table 2).

Highlights

- A methodology to estimate relative changes based on a pooled approach is proposed.
- Gridded relative changes for 24-h rainfall intensity update are obtained.
- Adjustments on relative changes are proposed for facilitating their application.
- The approach is applied to Canada.

Abstract

The potential effect of climate change needs to be considered in urban infrastructure design and risk assessment to improve reliability. The present study proposes a methodology for obtaining grid-scale relative changes for updating 24-h extreme rainfall intensity, through the estimation of rainfall intensity quantiles from baseline and future simulations using a pooled frequency analysis approach. Coherence of relative changes over return periods and time horizons is analysed, and adjustments are proposed to facilitate the application of relative changes in practice. The approach is applied to Canada, using gridded daily precipitation series from model combinations belonging to the North American Coordinated Regional Climate Downscaling Experiment. Multi-model 10^{th}, 50^{th} and 90^{th} percentile relative changes are provided for six return periods, considering two future scenarios (RCP 4.5 and RCP 8.5), and two horizons (2050 and 2080). Overall, estimated relative changes varied smoothly and formed a number of clusters of similar values across the country. Relative changes for RCP 8.5 are recommended for 2050, whereas either those for RCP 4.5 or RCP 8.5 could be used for 2080. As an example, median multi-model 50th percentile relative change over Canada is found to be 14%, 16% and 27% for RCP 4.5 – 2080, RCP 8.5 – 2050, and RCP 8.5 – 2080, respectively.

Declaration of interests

☒ The authors declare that they have no known competing financial interests or personal relationships that could have appeared to influence the work reported in this paper.

☐The authors declare the following financial interests/personal relationships which may be considered as potential competing interests: